

A New Robotic Uterine Positioner for Laparoscopic Hysterectomy with Passive Safety Mechanisms: Design and Experiments

Hiu Man Yip, Zerui Wang, David Navarro-Alarcon, Peng Li, Yun-hui Liu and Tak Hong Cheung

Abstract—In this paper, we present a new robotic uterine positioner for total laparoscopic hysterectomy. The robot is designed to actively position the patient's uterus during surgery, a lengthy and tedious task that is traditionally performed by a human assistant. Safety is simply the most important concern when developing robots for surgical purposes; we address this concern in the design of our robot from a mechanical perspective. To this end, we develop a 3-DOF robotic uterine positioner with an in-body remote center of motion (RCM); this key feature allows to prevent injuries to the patient when large motions occur at the cervix. A linearly-actuated arc-guided RCM mechanism is introduced to guarantee the rigidity and stability of the robot; The system's design allows to manipulate the uterus in a decoupled manner, thus control complexity can be reduced. Passive safety mechanisms are also implemented in all DOF of the robot in order to limit the interaction forces with the patient. Experiments, including an ex-vivo test conducted with cadaver, are conducted to verify the robot's performance.

I. INTRODUCTION

Hysterectomy is a commonly performed gynecological procedure on which the uterus of the patient is surgically removed. When performing total laparoscopic hysterectomy (TLH), no matter the surgery is performed in a traditional or robot-assisted (e.g. with the daVinci system) way, an assistant is usually needed to manipulate the patient's uterus by mean of a passive positioner. For traditional laparoscopic hysterectomy, the operative time generally lasts around 120 minutes [1]; for a robot-assisted one, it usually lasts no less than 190 minutes [2], [3]. Throughout the operation, the assistant is asked to continuously position the patient's uterus, this may easily cause fatigue to the assistant and eventually affect the manipulation performance and threaten the patient. Furthermore, the efficiency of current robot-assisted laparoscopic hysterectomy is not yet comparable with that of the traditional procedure. In terms of both safety and efficiency, it is worth keeping the primary surgeon to directly perform the procedure. Thus, it is reasonable to introduce a robot, which is fatigue-free, to take up the task of the uterus positioning assistant. This also helps to save the valuable manpower in the operating theater.

Surgical robots can mainly be classified into two types [4], surgeon extenders (e.g. ZEUS [5], daVinci surgical system [6]) which supplement the surgeon's ability in tool

This work is supported in part by the RGC (grant numbers: 415011, CUHK6/CRF/13G) and ITF (grant number: ITS/020/12FP) of HKSAR.

H.M. Yip, Z. Wang, D. Navarro-Alarcon, P. Li and Y.-H. Liu are with the Department of Mechanical and Automation Engineering, T.H. Cheung is with the Department of Obstetrics and Gynaecology, the Chinese University of Hong Kong, HKSAR. (e-mail: hmyip@mae.cuhk.edu.hk)

manipulation and assistive surgical robots which provide auxiliary supports.

A common task of assistive surgical robots is endoscope manipulation (e.g. AESOP [7], LARS [8], EndoAssist [9]). Examples other than endoscope manipulators include the RIO robotic arm designed for orthopedic surgeries [10] and ViKY UP [11] targeted on uterus positioning in laparoscopic hysterectomy.

When developing robots for medical purposes, safety is an important issue to be addressed. In general, safety of a robot can be improved with both active and passive approaches. Active safety control highly depends on the control algorithm; threats exist once the controller fails. Thus, to protect the patient from injuries, passive safety protection approaches which work regardless of whether the controller works or not is a highly desirable feature.

Remote center of motion mechanism [12] is a widely used approach among medical robots to constraint the motion of a certain point in the workspace, (see e.g. [13]–[15]). Note that the vast majority of existing medical robots are designed for tool manipulation during laparoscopic surgeries, which leads to designs that placing the RCM directly at the entry port on patient's abdomen. However, in our uterus positioning application, an in-body RCM located at the patient's cervix is preferred due to the human anatomic constraint, on which large motions at the cervix must be avoided to prevent injuries.

Though ViKY UP [11] has been applied for uterus positioning, it has an RCM located at the entry point of the vagina, which may not be optimal (note that the tissues on the vagina are more flexible to small motions than the ligaments on the cervix). Moreover, the system generates a cone-shaped shaped workspace which requires joint coordination when performing typical uterus manipulation motions, this increases the control complexity.

A robotic prototype for hysterectomy was developed in [16]. This system is capable of providing an in-body RCM located at the cervix and has decoupled joint motions. However, due to its open-ended arc structure, vibrations occur during manipulation. Under-bed space is also needed for installing the robot, which brings limitations in adapting the robot to operating tables with different designs.

A. Contribution

In this paper, we present a new robotic uterine positioner developed for laparoscopic hysterectomy. Safety is emphasized in the design of our robot. Methods to improve safety include: (1) the existence of an in-body RCM located at the

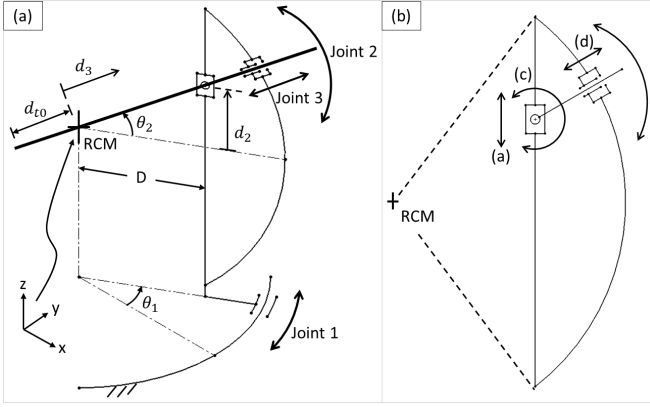


Fig. 1. The kinematic diagram of the robotic system. (a) The 3-DOF robotic system. (b) The LAAG RCM mechanism.

patient's cervix; (2) the introduction of a linearly-actuated arc-guided RCM mechanism which improves the robot's rigidity; (3) decoupled joint motion for manipulation which reduces control complexity; and (4) the use of passive safety mechanisms which limit the interaction force between the patient and the robot. Experiments including an ex vivo test are conducted to verify the performance of the robotic prototype.

II. DESIGN OF ROBOT

In this section, we present the design of the robot. The mechanisms used, kinematics of the robot, the mechanical design and details of its control system are provided.

A. Working Principle and Mechanism

Fig. 1(a) shows the kinematic structure of our 3-DOF robotic system. In this paper, we denote the yaw joint by joint 1, pitch joint by joint 2 and insertion joint by joint 3.

In our design, joint 1 is an element sliding along an arc-shaped guide; Joint 2 is mounted onto the sliding element of joint 1. It provides an arc-shaped trajectory similar to joint 1 through a linearly-actuated arc-guided (LAAG) RCM mechanism, which will be presented in Section II-B; Joint 3 is merged to the output element of joint 2. It is a standard prismatic joint which allows translation along a linear trajectory.

Both mechanisms used for joint 1 and joint 2 are single-DOF RCM mechanisms which give an RCM located at the center of their corresponding arc-shaped guide. To merge these RCMs together to give an overall RCM aligning with the surgical tool mounted to the robot, the following constraints are fulfilled in our design:

- The axis of rotation of joint 1 must intersect the RCM of the output trajectory of joint 2.
- The axis of translation of joint 3 must lie on the normal of the output trajectory of the joint 2 and pass through the common RCM.
- The motion plane of the joint 1 must be perpendicular to the motion plane of the joint 2.

This 3-DOF RCM mechanism is particularly designed and is suitable for an assistive surgical robot which helps in uterus positioning during laparoscopic hysterectomy. With this design, the RCM can be placed at (or close to) the cervix of the patient, which is inside the patient's body, as there exist enough space between the robot links and the RCM. For laparoscopic hysterectomy, it is more desirable to have the RCM (which remains stationary throughout the manipulation) placed at the cervix due to the anatomic constraint that large motions at the cervix are prohibited.

Manipulation of the uterus can be achieved in a decoupled manner with the joint motions and workspace provided by this 3-DOF RCM mechanism, which makes control easier and reduces the potential errors caused by joints-coordination control. By purely moving joint 1, lateral manipulation of uterus can be achieved; By moving joint 2, anteversion/retroversion of uterus can be achieved; To apply tension to the uterus, it can be simply achieved by moving joint 3.

This mechanism increases the feasibility and easiness of setting up the robot in the operating theater. In this design, space along the vertical axis of the RCM is reserved, all links of the robot are suppressed away from this area. This makes the set up easier as no part of the robot would interfere with the operating table. No space under or above the the operating table is required for the setup.

B. The Linearly-Actuated Arc-Guided Mechanism

A linearly-actuated arc-guided (LAAG) RCM mechanism is designed to generate motion of the pitch joint (joint 2). This mechanism is designed to provide good rigidity and hence the stability to the robot.

Fig. 1(b) shows the kinematic diagram of the LAAG RCM mechanism. The mechanism consists four major components, an active element (a) and three passive elements (b-d).

Element (a) is actively driven by an actuator to move along a vertical trajectory and it drives the output element (b) which is forced to follow an arc-shaped trajectory via a revolute joint (c) and a prismatic joint (d). As elements (a) and (b) are moving in two different trajectories, to drive one by the other, motion compensation is needed and thus elements (c) and (d) are introduced to connect elements (a) and (b).

The elements construct a closed-loop linkage mechanism which eliminates non-rigid opened-loop cantilever structure, and gives an RCM located at the center of the arc-shaped guide which element (b) is forced to move along. Assume the whole mechanism to be 2-dimensional and a rod-shaped surgical tool is mounted to element (b) and the tool is forced to lie on the normal of the arc-shaped guide, then, the RCM would always lie on the axial direction of the surgical tool.

If this mechanism is the only DOF of a system, the actuator for driving element (a) can be statically installed on the base link by choosing a proper driving mechanism (e.g. belt-and-pulley mechanism, ball-screw mechanism). This provides an alternative to tendon-driven mechanisms, which frequently suffers from having loose tendon and often needs maintenance. In [17], the authors have proved that the

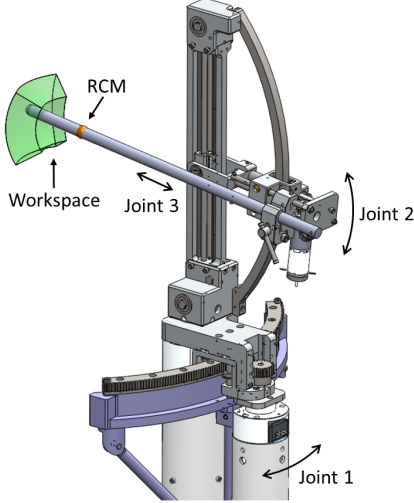


Fig. 2. The CAD model of the robotic system and its workspace.

LAAG mechanism is back-drivable, which is an important property that improves safety.

C. Kinematics

In this section, we present the kinematics and workspace of the 3-DOF robotic system. To model the kinematics, we assume the surgical tool (in shape of a straight rod) is mounted to joint 3. Refer to Fig. 1, we define that the origin of the right-handed world coordinate frame is located at the RCM. In the figure, θ_1 denotes the angle of rotation of the joint 1; d_2 denotes the displacement of the linear element of the joint 2; D denotes the distance between the RCM and the axis of translation of the linear element of the joint 2; $\theta_2 = \tan^{-1}(\frac{d_2}{D})$ denotes the angle of rotation of the joint 2; d_3 denotes the displacement of the joint 3; and d_{t0} denotes the initial distance between the tip of the surgical instrument and the RCM.

The position of the end-effector \mathbf{p}_t in the Cartesian space is given by:

$$\mathbf{p}_t = \begin{bmatrix} -(d_{t0} - d_3)\cos\theta_2\cos\theta_1 \\ -(d_{t0} - d_3)\cos\theta_2\sin\theta_1 \\ -(d_{t0} - d_3)\sin\theta_2 \end{bmatrix} \quad (1)$$

From Eq. 1, we can see that the robotic system provides a partial spherical workspace centered at the RCM with its radius varying from d_{t0} to $d_{t0} - d_3$. The workspace of the robotic system is graphically illustrated in Fig. 2.

D. Design and Prototyping

The robot is designed based on the kinematic diagram presented in Section II-A. Fig. 2 shows the CAD model of the robot. To improve safety, all joints of the robot are designed to be back-drivable. That is, the joints can be manually moved when necessary if electricity power is cut off. When comparing with self-locked driving mechanisms, back-drivable mechanisms can also reduce the chance of

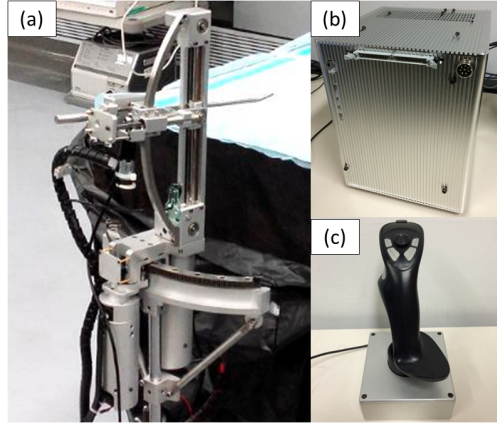


Fig. 3. The prototype of the robotic system. (a) The robot. (b) The controller. (c) The joystick interface

applying unnoticeable excessive driving force that may injure the patient.

Joint 1 of the robotic system is realized by a pinion and rack mechanism, which is back-drivable. A 20W DC motor with passive safety mechanism implemented is used as its actuator. Details of this actuator would be introduced in Section II-E. To realize the motion, an arc-shaped guide with gear teeth on its outer ring is used to guide its joint motion. An actuated block with the motor and pinion installed is forced to move along the guide by gears meshing.

The mechanical components of joint 2 are installed on top of the actuated block of joint 1; its actuator is installed statically on this block. The same compliant actuator used in joint 1 is used as its actuator. To realize the LAAG RCM mechanism, a belt-and-pulley mechanism is used to drive the linearly-actuated element to provide back-drivability. A passive block sliding along a smooth arc-shaped guide acts as the output element. Motion compensation between the actuated and output elements is achieved by a hinge connected to the actuated block by mean of a pair of parallel rods which are allowed to pass through the output block.

The mechanical components of joint 3 are partially merged with the components of joint 2. A standard pinion-and-rack mechanism is used to realize the linear motion. A 6W DC motor with a pinion on its shaft is installed onto the output block of joint 2 while a cylindrical rack which meshes with the pinion is forced to slide inside the hollow rod of the hinge of joint 2. A pair of rods with a gripper (which later holds the surgical tool) mounted on them are connected in parallel to the rack through a metal plate to act as the output. Details of the passive safety mechanism implemented to limit the insertion force between the joint and its contacting environment are given in Section II-E.

The developed prototype is shown in Fig. 3.

E. Passive Safety Mechanisms

To prevent injuries to patient, passive safety mechanisms are implemented to limit the interaction forces between the patient and the robot. Joint 1 and joint 2 are driven by passive compliant actuators [18], as shown in Fig. 4. For joint 3, we

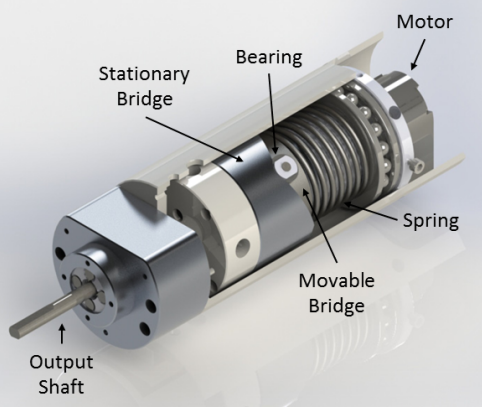


Fig. 4. CAD model of the compliant actuator with passive safety mechanism implemented.

implemented a passive mechanism similar to a tumbler-lock. With these devices, power transmission from the motors to the joints will be mechanically cut off if the interaction force exceeds the pre-defined safety thresholds.

The compliant actuator consists of two parts, a movable bridge which is only allowed to move along the axial direction of the motor, and a stationary bridge with a helicoid surface which is only allowed to rotate around the motor. Bearings are mounted on the movable bridge. In normal situations, the bearings are constrained to stay inside the slots of the stationary bridge, thus the output shaft of the compliant actuator can be driven by the motor. When the torque acting on the output shaft exceeds the pre-defined safety threshold, the bearings will be pushed away from the slots and slide along the helicoid surface. Thus, power transmission between the motor and the output shaft is mechanically cut off.

The working principle of the tumbler-lock passive safety mechanism is described in Fig. 5. In normal condition, the locking pin with a spherical tip (e.g. a ball plunger) is pressed into the slot of the shaft by the spring. However, when the interaction force exceeds the pre-defined threshold, the spring is compressed and the locking pin is pushed out from the slot. Thus, the gripper is allowed to slide along the shaft and motion transmitted from the shaft to the gripper is cut off.

In our design (Fig. 5), the triggering threshold of the mechanism can be adjusted to fit actual needs by using different ball plunger combinations.

F. Control System

The presented robot is controlled by a control system composed of a low-level industrial motion controller and a high-level PC-based controller (Fig. 3(b)). We use a Galil DMC-4040 4-axis industrial motion controller with embedded amplifiers as the low-level controller, which outputs the driving currents to the actuators. For the high-level controller, a Linux-based industrial PC (i5-3550S CPU, 4GB RAM, Intel H61 Chipset) is used. It processes all external inputs such as feedbacks from cameras, force sensor, the input commands from the user interface, and computes the corresponding motion control algorithms.

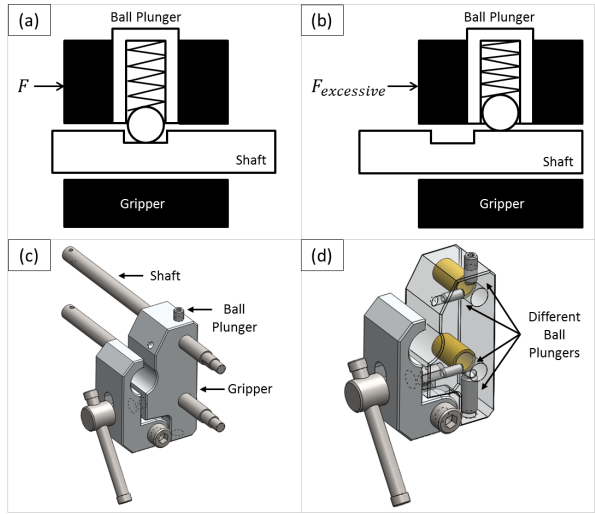


Fig. 5. The working principle of the tumbler-lock passive safety mechanism. (a) In normal condition. (b) The safety mechanism is triggered. (c) CAD model of the safety mechanism. (d) CAD model of the gripper showing that the use of different ball plunger combinations is allowed.

Communication between these high-level and low-level modules is established via a high-speed Ethernet connection; all the joints of the robot are commanded using velocity control mode with a standard PD control law.

III. EXPERIMENTS

In this section, we present the experiments conducted to verify the performance of the developed robot prototype.

A. Existence of an RCM

The robotic system is designed to have a common RCM among joints to improve safety. To verify the existence of such RCM, videos are recorded with a camera mounted onto a tripod. The robot is powered and controlled to give different motions and the motions of the prototype are observed.

In recording the videos, a uterine manipulator (with shape of a rod with an up-tilting tip) is used as the surgical tool. The existence of an RCM is proved by overlapping the frames captured from the videos. In Fig. 6, (a) to (c) shows the motion of joint 1, where (d) is obtained by overlapping (a) to (c); (e) to (g) shows the motion of joint 2, where (h) is obtained by overlapping (e) to (g); (i) to (k) shows the motion of joint 3, where (l) is obtained by overlapping (i) to (k). To obtain (m), we overlap (a), (e) and (i); To obtain (n), we overlap (b), (f) and (j); To obtain (o), we overlap (c), (g) and (k); To obtain (p), we overlap (a), (f) and (k). It can be observed that from each image obtained by overlapping, there exists a common intersection point, which is the RCM. To further verify that these intersection points from different images are common, a vertical dotted line is drawn to pass through the intersection points of (d), (h) and (l) and a horizontal dotted line is drawn to pass through the intersection points of (m), (n) and (o). These dotted lines intersect at (p) and this intersection point aligns with the RCM obtained in (p). This visualizes that our robotic system

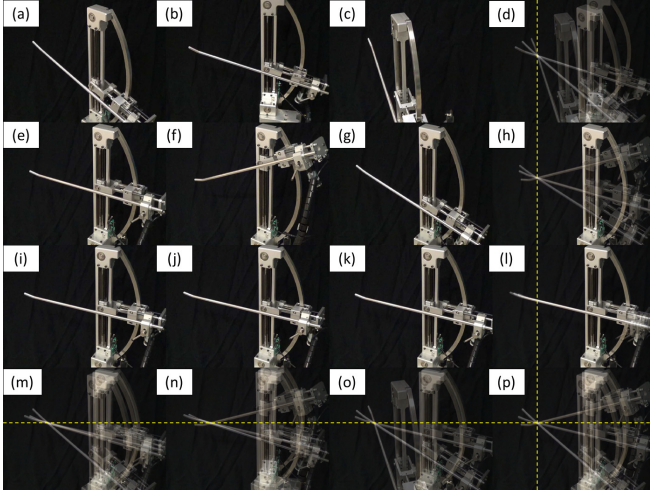


Fig. 6. Visualization of the existence of a common RCM.

does give a common RCM among joint 1, joint 2 and joint 3.

B. Joint Coordination Experiment

The performance of the robot in responding to an assigned input is tested in this experiment.

In this experiment, the robot is programmed to trace an elliptical trajectory on a vertical plane in the Cartesian space. As the robot is designed to have decoupled motions in the spherical coordinate system, when manipulating in the Cartesian space, coordination among joints is needed. Thus, in order to follow the given elliptical trajectory, all joints of the robot are required to simultaneously track their corresponding trajectories.

The elliptical trajectory assigned to the robot is as follows:

$$\mathbf{p}_d = [X \quad Y \sin \frac{2\pi}{P} t \quad Z \cos \frac{2\pi}{P} t]^T \quad (2)$$

where X , Y and Z are the constant manipulation amplitudes in the x , y and z Cartesian directions respectively, P is the time for completing one loop of the elliptical trajectory and t is the time variable.

In this experiment, we choose $X = X_0$, where X_0 is the initial position of the end-effector in the x -direction before the tracking experiment starts, $Y = -40$ mm, $Z = -20$ mm and $P = 10$ seconds. Desired joint velocity profiles fed to the robot are computed with a standard Jacobian-based kinematic controller:

$$\dot{\mathbf{q}} = -\lambda \mathbf{J}^{-1}(\mathbf{q})(\mathbf{p} - \mathbf{p}_d) \quad (3)$$

where $\dot{\mathbf{q}}$ is the joint velocity vector, λ is a positive feedback scalar and \mathbf{p} is the measured position of the end-effector in the Cartesian space.

Fig. 7 shows the experimental tracking results of individual coordinates/joints in both the Cartesian and joint spaces. In the figure, the black line presents the desired trajectory to be followed while the red line shows the measured trajectory followed by the robot.

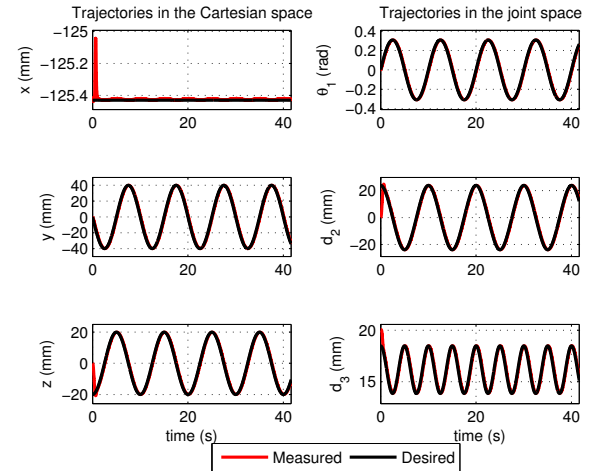


Fig. 7. Tracking results of individual coordinates/joints in the Cartesian space (left) and the joint space (right).

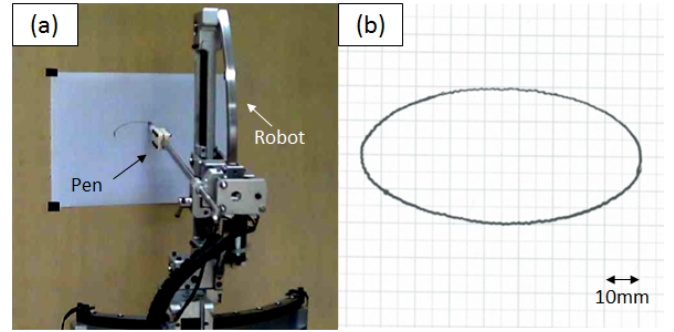


Fig. 8. Experimental setup for visualizing the output trajectory. (a) Experimental setup. (b) Pattern obtained from the grid paper.

From the results, it can be observed that our robot is capable of closely following the assigned trajectory profile. Consider the tracking results after saturation (e.g. after 2 seconds), in the Cartesian space, the mean absolute errors of the x -, y - and z -axis are 0.0046 mm, 1.6 mm and 0.81 mm respectively; In the joint space, the mean absolute errors of joint 1, joint 2 and joint 3 are 0.013 rad, 0.97 mm and 0.19 mm respectively.

To externally evaluate the accuracy of the system, a marker pen is mounted to the robot as the end-effector. A wooden board with a piece of grid paper attached is put vertically in front of the robot to act as the output plane. Fig. 8(a) shows the experimental setup and Fig. 8(b) shows the result obtained.

C. Uterus Manipulation Experiment

The robotic system is developed to assist in positioning the patient's uterus during hysterectomy. Here, we demonstrate the application of the robot with a female pelvic manikin.

Motions of independent joints of the robot can be referred to Fig. 6 and the description in Section III-A. As the robot is intentionally designed to allow uterus manipulation to be achieved in a decoupled manner, by solely moving joint 1 to joint 3 respectively, lateral manipulation of uterus (see

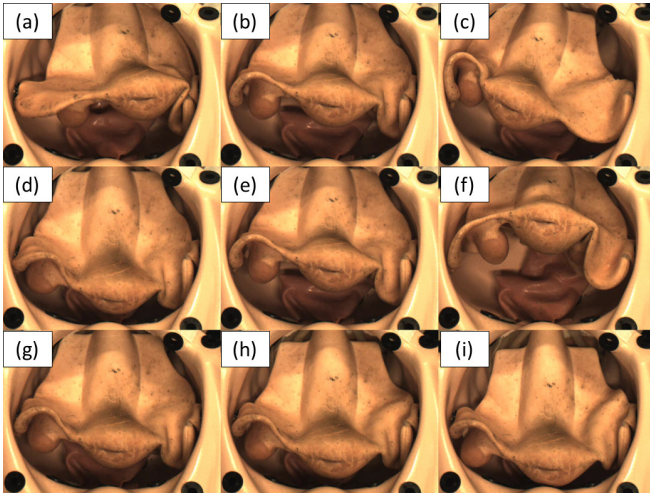


Fig. 9. Applying the robot on a manikin. (a)-(c) Lateral manipulation. (d)-(f) Anteversion and retroversion. (g)-(i) Tensioning.

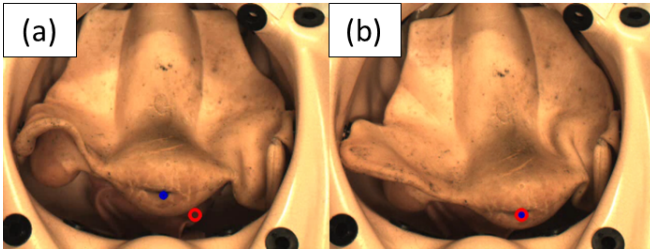


Fig. 10. The task assigned to the human user during the human-in-loop manipulation experiment. (a) Before reaching the target. (b) Reached the target.

Fig. 9(a) to (c)), anteversion and retroversion of uterus (see Fig. 9(d) to (f)), and tensioning of uterus (see Fig. 9(g) to (i)) can be performed with the assistance of our robot.

D. User-controlled Manipulation

To verify the robot's performance in assisting the user to perform the specified task, a user-in-loop uterus manipulation experiment is conducted. In this experiment, the surgical scenario is simulated with a female pelvic manikin and a CCD camera. The user is asked to control the robot through the joystick interface (Fig. 3(c)) and manipulate a reference point on the manikin's uterus (represented by a blue dot) to some desired image positions (represented by a red circle) based on the image feedback from the camera (Fig. 10).

These randomly selected target image positions are programmed to appear one by one. The user is asked to align the blue dot with the red circle as close as possible. Based on the user's judgment, once the target position is reached, a new target position would appear, so on and so forth.

The experimental results are presented in Fig. 11. The red line represents the target image position profile while the blue line represents the actual manipulation trajectory. In this plot, the position profile is separately described by its x- and y-coordinates on the image. It can be observed that the reference point always tends to reach the desired target position every time when the target is changed.

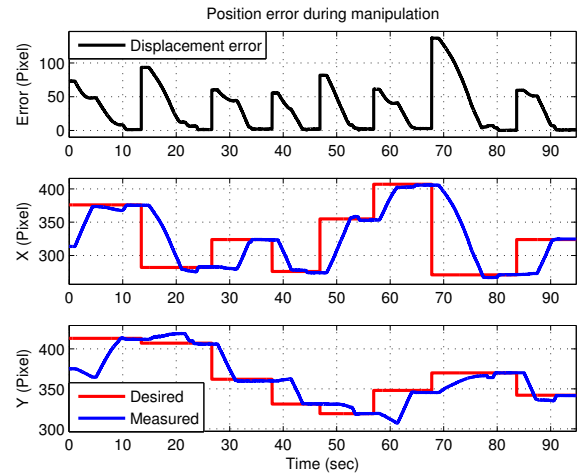


Fig. 11. Position error during the manipulation experiment.

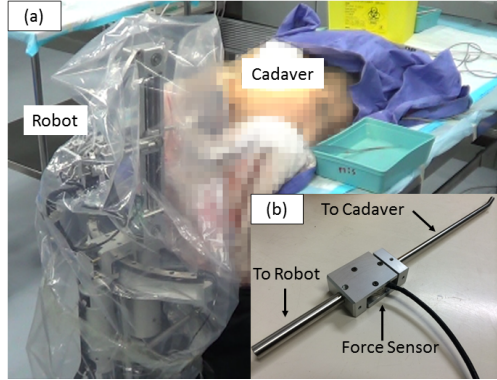


Fig. 12. Setup of the ex vivo experiment. (a) The experimental setup. (b) The force measuring uterine manipulator.

The black line of the plot represents the absolute pixel displacement error. It describes the distance between the target image position and the reference point being manipulated. It can be observed that the error has the tendency of converging to a value close to zero before each new target position is specified.

This experiment shows that our robot is controllable by a human user, the user can manipulate the uterus to some randomly selected target positions with the assistance of the robot, which is the purpose of the developed robotic system.

E. Ex vivo Experiment

To verify the performance of the robot in a more realistic environment, an ex vivo experiment is conducted with a human pelvic cadaver at the Prince of Wales Hospital in Hong Kong. The experimental setup is shown in Fig. 12(a). We set up the robot as what it should be when it is applied to a real surgery, but, instead of applying to a patient, we apply our robot to a cadaver. Uterus manipulation is then done with the assistance of the robot following the joystick commands given by the surgeon. In Fig. 12, the robot is covered by a plastic bag to avoid contaminations and the cadaver is intentionally blurred.

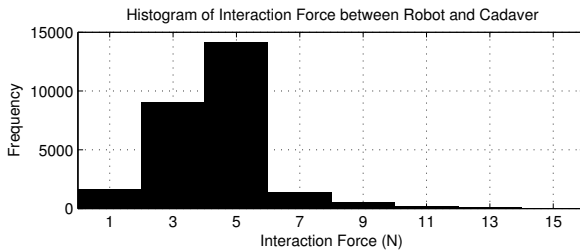


Fig. 13. A histogram showing the measured interaction force between the robot and the cadaver during the ex vivo experiment.

The objectives of this experiment are (1) to verify that the robot can be applied to a realistic application and (2) to estimate the interaction force between the human body and the uterine manipulator (this way, the pre-defined triggering threshold for the passive safety mechanisms can be estimated).

To measure the interaction force, a uterine manipulating tool (similar to the one from Apple Med) is instrumented with a force/moment transducer (see Fig. 12(b)). We use an ATI Mini40 6-axis force/torque sensor for this task.

During the 45-minute ex vivo experiment, the interaction force between the robot and the cadaver is continuously measured. In this experiment, we set the sampling time interval to 0.1 second. A histogram showing the magnitude of the interaction force throughout the experiment is presented in Fig. 13. The results show that, on average, the interaction force is within the range of 2N to 6N; the maximum applied force varies around 14N to 16N. These data may serve as one of the references when designing the triggering thresholds of the passive safety mechanisms for practical applications.

IV. CONCLUSION

In this paper, we presented a 3-DOF robotic system designed for uterus positioning during laparoscopic hysterectomy. Safety issues are emphasized in the design from a mechanical perspective.

An in-body RCM mechanism is adopted to provide an always stationary point at the patient's cervix during manipulation. This helps to prevent any accidental injuries to the patient caused by prohibited movements at the cervix. In addition, a linearly-actuated arc-guided RCM mechanism is introduced to enable the pitch motion of the robot. Open-looped arc structure is eliminated with this mechanism and the rigidity and hence the reliability of the robot is improved. Besides, the robot is designed to perform uterus manipulation in a joint decoupled manner thus control complexity can be reduced. Furthermore, passive safety mechanisms are implemented to all joints to limit the interaction force between the robot and the patient. This prevents the patient from unnecessary injuries due to excessive forces being exerted.

Various experiments have been conducted to verify the robot's performance. Experimental results show that the robot is capable of performing the required positioning task. In the future, to further improve the safety of the robot, clinical trials which measure the real force applied by the

surgeon during uterus positioning in traditional surgeries are expected. Besides limiting the interaction force, safety can also be improved by limiting the moving ranges of the robot; clinical trials for determining these proper ranges are also recommended.

REFERENCES

- [1] D. J. Shimizu, in *Hysterectomy: procedures, complications, and alternatives*, D. J. Shimizu, Ed. New York, NY, USA: Nova Science Publishers, Inc., 2011, pp. 102–103, 146–147, 176–177.
- [2] R. K. Reynolds and A. P. Advincula, "Robot-assisted laparoscopic hysterectomy: technique and initial experience," *The American Journal of Surgery*, vol. 191, pp. 555–560, 2006.
- [3] T. M. Beste, K. H. Nelson, and J. A. Daucher, "Total laparoscopic hysterectomy utilizing a robotic surgical system," *Journal of the Society of Laparoendoscopic Surgeons*, vol. 9, pp. 13–15, 2005.
- [4] R. Taylor, "A perspective on medical robotics," *Proceedings of the IEEE*, vol. 94, no. 9, pp. 1652–1664, Sept 2006.
- [5] H. Reichensperger *et al.*, "Use of the voice-controlled and computer-assisted surgical system zeus for endoscopic coronary artery bypass grafting," *The Journal of Thoracic and Cardiovascular Surgery*, vol. 118, pp. 11–16, July 1999.
- [6] G. Guthart and J. Salisbury, J., "The intuitivetm telesurgery system: overview and application," in *Robotics and Automation, 2000. Proceedings. ICRA '00. IEEE International Conference on*, 2000, pp. 618–621 vol.1.
- [7] J. M. Sackier and Y. Wang, "Robotically assisted laparoscopic surgery," *Surg Endoscopy*, vol. 8, pp. 63–66, 1994.
- [8] R. Taylor *et al.*, "A telerobotic assistant for laparoscopic surgery," *Engineering in Medicine and Biology Magazine, IEEE*, vol. 14, no. 3, pp. 279–288, 1995.
- [9] S. Aiona *et al.*, "Controlled trial of the introduction of a robotic camera assistant (endoassist) for laparoscopic cholecystectomy," *Surg Endoscopy*, vol. 16, pp. 1267–1270, 2002.
- [10] J. H. Lonner, T. K. John, and M. A. Conditt, "Robotic arm-assisted uka improves tibial component alignment: a pilot study," *Clinical Orthopaedic and Related Research*, vol. 468, pp. 141–146, 2010.
- [11] K. Swan, J. Kim, and A. Advincula, "Advanced uterine manipulation technologies," *Surgical Technology International*, vol. 20, pp. 215–220, 2010.
- [12] C.-H. Kuo and J. Dai, "Robotics for minimally invasive surgery: a historical review from the perspective of kinematics," in *International Symposium on History of Machines and Mechanisms*, H.-S. Yan and M. Ceccarelli, Eds. Springer Netherlands, 2009, pp. 337–354.
- [13] N. Zemiti, G. Morel, T. Ortmair, and N. Bonnet, "Mechatronic design of a new robot for force control in minimally invasive surgery," *Mechatronics, IEEE/ASME Transactions on*, vol. 12, no. 2, pp. 143–153, 2007.
- [14] J. Rosen, M. Lum, M. Sinanan, and B. Hannaford, "Raven: developing a surgical robot from a concept to a transatlantic teleoperation experiment," in *Surgical Robotics*, R. M. S. Jacob Rosen, Blake Hannaford, Ed. Springer, 2011, pp. 159–197.
- [15] G. Buess *et al.*, "A new remote-controlled endoscope positioning system for endoscopic solo surgery. the fips endoarm," *Surg Endoscopy*, vol. 24, pp. 395–399, Apr. 2000.
- [16] H. M. Yip, P. Li, D. Navarro-Alarcon, and Y. H. Liu, "Towards developing a robot assistant for uterus positioning during hysterectomy: system design and experiments," *Robotics and Biomimetics*, vol. 1, no. 9, 2014.
- [17] H. M. Yip, P. Li, D. Navarro-Alarcon, and Y.-H. Liu, "A new circular-guided remote center of motion mechanism for assistive surgical robots," in *Robotics and Biomimetics (ROBIO), 2014 IEEE International Conference on*, Dec. 2014, pp. 217–222.
- [18] Z. Wang *et al.*, "Design and control of a novel multi-state compliant safe joint for robotic surgery," in *Robotics and Automation (ICRA), 2015 IEEE International Conference on*, May 2015, pp. 1023–1028.